Miniaturized Spurious Passband Suppression Microstrip Filter Using Meandered Parallel Coupled Lines

Shih-Ming Wang, Chun-Hsiang Chi, Ming-Yu Hsieh, and Chi-Yang Chang, *Member, IEEE*

***Abstract*—A novel meandered parallel coupled-line structure is proposed to suppress the first spurious passband of a microstrip bandpass filter. The meandered parallel coupled line can equalize the modal transmission phases at any interested frequency such as first spurious passband frequency due to its dispersive response. Several filters are designed and fabricated on a substrate with a dielectric constant of 10.2 and a thickness of 50 mil (1.27 mm) to demonstrate the validity of the proposed method. The example filters are chosen to be of large fractional bandwidth and with a relatively high dielectric-constant substrate where, in these cases, the first spurious passband near twice of the passband frequency $(2f_o)$ seriously degrades the conventional parallel coupled filter's upper stopband performance. The upper stopband performance of the proposed filters drastically improves that the measured first spurious passband are suppressed to better than −50 dB for all example filters. Besides, a meandered coupled line not only suppresses the filter's first passband, but also largely shrinks its length. The characteristics of the proposed structure and the design procedures of the filter are described in detail.**

***Index Terms*—Microstrip, microwave filter, parallel coupled line, spurious passband.**

I. Introduction

THE MICROSTRIP parallel coupled filter first proposed by Cohn in 1958 [1] has been widely used in many microwave and wireless communication systems. This type of filter is popular due to its planar structure, insensitivity to fabrication tolerance, wide realizable bandwidth (from a few percent to more than 60%) [2]–[4], and simple synthesis procedures [5]. However, there are several disadvantages of the conventional microstrip parallel coupled filter. One of the disadvantages is that the first spurious passband of this type of filter appears at twice of the basic passband frequency $(2f_o)$. Therefore, the rejection of the upper stopband is worse than that of the lower stopband. Sometimes, the upper stopband rejection may be as bad as −10 dB, especially in case of wide bandwidth filters. Another disadvantage is the whole length of the filter is too long, especially when the order of a filter becomes high. Both disadvantages greatly limit the application of this type of filter.

The reason for the first spurious passband is that the even-mode phase velocity is always slower than that of the odd mode because of the inhomogeneous medium of microstrip structure. The unequal modal phase velocities at $2f_o$ cause the first spurious passband. There are two basic methods to equalize the modal transmission phase: providing different lengths for the even and odd mode, or equalizing the modal phase velocities. In [6] and [7], an over-coupled resonator is proposed to extend the electrical length of the odd mode to compensate the difference in the phase velocities. The structure in [8] and [9] uses capacitors to slow down the odd-mode phase velocity. The substrate suspension structures in [10] are substantially designed to speed up the even-mode phase velocity, and make the modal phase velocities equal. The wiggly coupled microstrip filter in [11] is also effective in improving the rejection characteristics of the filter at $2f_o$. These published filters have some drawbacks. Firstly, all these filters in [6]–[11] are too long due to their straight structure, especially when the order of the filter becomes high. The filters in [8] and [9] need extra circuit components that cause higher material and assembly cost. The filter in [10] needs to suspend the substrate, and a costly package is required. The filters in [6], [7], [10], and [11] are with complex design procedures.

An alternative method to eliminate spurious passband is to use a self-filtering resonator [12] where the resonator is formed by a high–low impedance low-pass filter. This kind of resonator is complex to layout as a parallel coupled filter. Moreover, due to the limitation of the high–low impedance ratio of the resonator, the spurious passband suppression is usually limited, unless a three-dimensional structure is used.

Another method to improve a parallel coupled filter's upper stopband performance is to move the first spurious passband away from $2f_o$ [13], [14]. Usually, using the step impedance resonator can shift the first higher order resonant frequency of a resonator. However, the step impedance method is to move, not to suppress, the first spurious band. If we want to move the first spurious passband to $3f_o$, a large impedance stepping ratio of the resonator is required and the layout of the filter becomes difficult.

In this paper, the motivation of the proposed filter is from [15] in that the even-mode phase velocity can be speeded up for a meandered parallel coupled line. As a parallel coupled filter meandered properly, not only can the filter's first spurious passband near $2f_o$ be suppressed, but also its size can be drastically reduced. It is also unprecedented that a parallel coupled filter

Manuscript received March 15, 2004. This work was supported in part by the National Science Council, R.O.C., under Grant NSC 92-2213-E-009-080.

S.-M. Wang, C.-H. Chi, and C.-Y. Chang are with the Department of Communication Engineering, National Chiao Tung University, Hsinchu 300, Taiwan, R.O.C. (e-mail: wsm.cm90g@nctu.edu.tw; kavh.cm91g@nctu.edu.tw; mhchang@cc.nctu.edu.tw).

M.-Y. Hsieh was with the Department of Communication Engineering, National Chiao Tung University, Hsinchu 300, Taiwan, R.O.C. He is now with the Chung-Shan Institute of Science and Technology, Lung-Tang 325, Taiwan, R.O.C. (e-mail: yoho.cm90g@nctu.edu.tw).

Digital Object Identifier 10.1109/TMTT.2004.840619

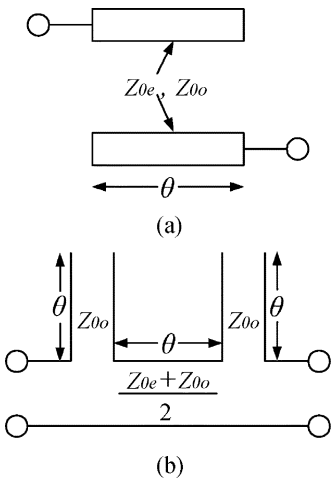

Fig. 1. TEM parallel coupled bandpass section. (a) Schematic representation. (b) Equivalent circuit.

can simultaneously suppress the spurious passband and greatly reduce its size. Furthermore, the proposed structure needs no additional circuit components or fabrication process such as capacitors or via-holes, thus, low fabrication cost can be kept.

The proposed filter is developed by meandering each parallel coupled section of the conventional parallel coupled filter. The new parallel coupled section can be modeled as a meandered parallel coupled line and a commercial circuit simulator can analyze it. In this paper, the behaviors of the meandered parallel coupled line are explained particularly. Systematic design procedures of the proposed filter are described in detail. Several meandered parallel coupled microstrip filters are fabricated with various specifications, and the measured results match well with simulation.

This paper is organized as follows. Section II explores the modal transmission phase equalization for a meandered parallel coupled microstrip line. Section III describes the design procedures of the proposed filter. Section IV presents the simulated and measured results of several fabricated filters. Section V discusses the transmission zeros in the upper stopband, and Section VI draws a conclusion.

II. Equalizing Modal Transmission Phases Using Meandered Parallel Coupled Line

The schematic of a parallel coupled bandpass section is shown in Fig. 1(a), and its equivalent circuit proposed by Matthaei [2] is shown in Fig. 1(b), where Z_{0e} and Z_{0o} are the even- and odd-mode characteristic impedances. The coupled electrical length θ, even-mode transmission phase θ_e, and odd-mode transmission phase θ_o are given by

$$\theta = \frac{(\theta_e + \theta_o)}{2} \tag{1}$$

$$\theta_e = \frac{\omega L}{V_p^e} \tag{2}$$

$$\theta_o = \frac{\omega L}{V_p^o} \tag{3}$$

where ω is the operating frequency, L is the physical length of the parallel coupled line, and V_p^e and V_p^o are the even- and odd-mode phase velocities. Here, the equivalent circuit in Fig. 1(b) is based on the TEM mode, and θ_e and θ_o are both equal to θ for all frequencies. From Fig. 1(b), at $2f_o$, because $\theta_e = \theta_o = 180°$, the series open stub will be open circuited at its input end. The transmission line between the two series open stubs is now at its half-wavelength resonant frequency where the first spurious passband locates. Since the two series open stubs are open circuited at their ends, no energy can be coupled to the half-wave resonator and a stopband will be formed. Therefore, the ultimate target of spurious passband suppression, described in Section I, is to achieve $\theta_e = \theta_o = 180°$ at $2f_o$. Unfortunately, in a microstrip structure, because the even-mode phase velocity of a microstrip coupled line is always slower than that of the odd-mode, θ_e is always larger than θ_o for all frequencies. Therefore, the spurious passband of a conventional microstrip parallel coupled filter at $2f_o$ occurs.

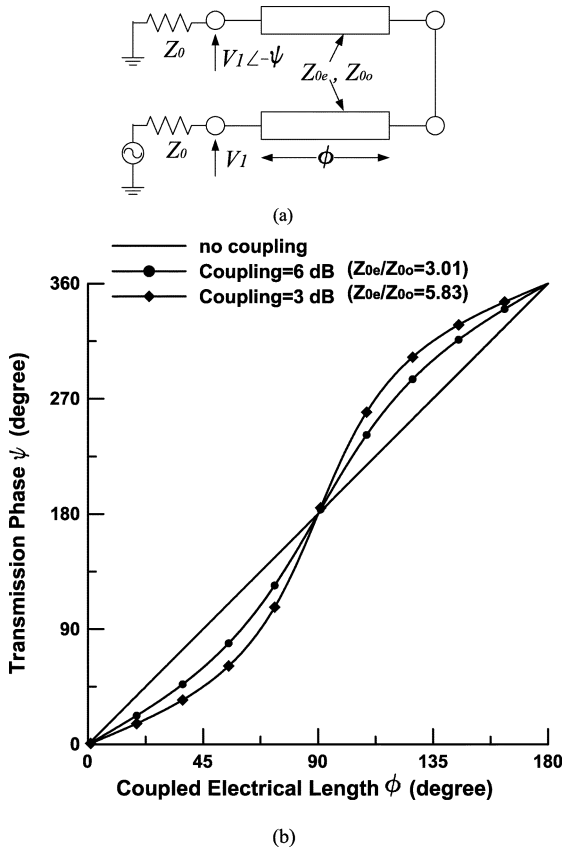

Fig. 2. Schiffman section. (a) Schematic representation. (b) Dispersive phase responses.

To understand the phase-equalizing scheme of the proposed structure, the behaviors of a Schiffman section must be studied. The Schiffman section, as shown in Fig. 2(a), is a two-port network, which is formed by connecting one side of a parallel coupled line [16]. If the interconnecting line has zero transmission phase, the relation between transmission phase ψ and coupled electrical length ϕ of the two-port network is determined by

$$\cos\psi = \frac{\left[\left(\frac{Z_{0e}}{Z_{0o}}\right) - \tan^2\phi\right]}{\left[\left(\frac{Z_{0e}}{Z_{0o}}\right) + \tan^2\phi\right]}. \tag{4}$$

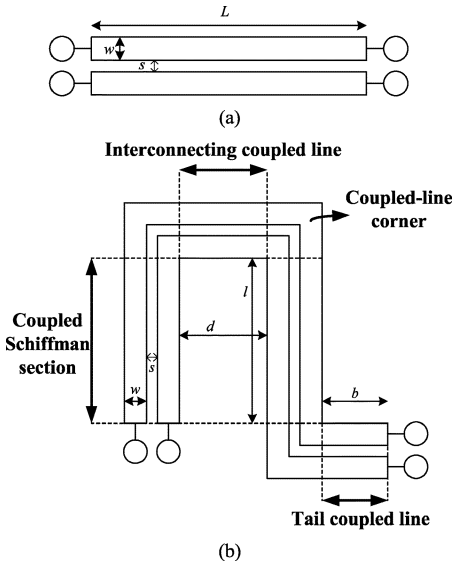

Fig. 3. (a) Conventional parallel coupled line. (b) Proposed meandered parallel coupled line.

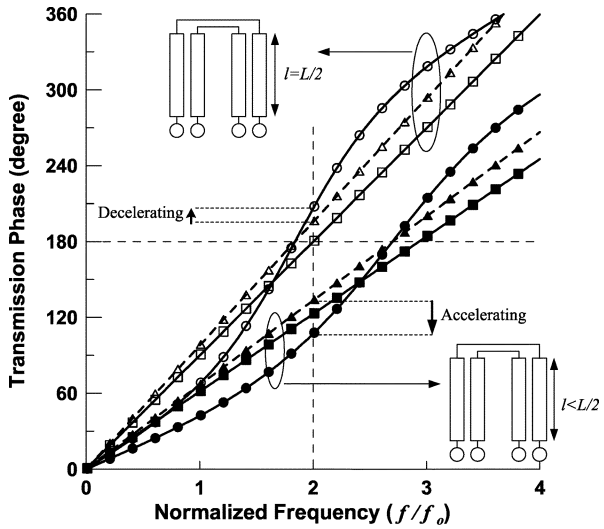

Fig. 4. Modal transmission phases of a conventional parallel coupled line and a coupled-Schiffman section with different coupled line lengths. For $l = L/2$, —□—: θ_o, —△—: θ_e without Schiffman effect, —○—: θ_e with Schiffman effect. For $l < L/2$, —■—: θ_o, —▲—: θ_e without Schiffman effect, —●—: θ_e with Schiffman effect.

From (4), the dispersive phase responses can be shown in Fig. 2(b). Fig. 2(b) clearly indicates that, as two lines couple to each other, the transmission phase ψ is reduced and, equivalently, the phase velocity is speeded up for $\psi < 180°$. The frequencies around $\psi = 90°$ have the largest accelerating ratio.

However, the meandered parallel coupled line is a four-port rather than a two-port circuit. As discussed in [15], when the meandered coupled line is excited with an even mode, it can be equivalent to a single-line Schiffman section because the even-mode modal current distribution is similar to that of a single line. Therefore, the even-mode phase velocity is accelerated when even-mode transmission phase $\theta_e < 180°$. To distinguish it from the conventional Schiffman section, we call it a coupled-Schiffman section.

Fig. 3(a) shows a conventional parallel coupled-line section. Fig. 3(b) depicts the proposed meandered parallel coupled-line section, which is the basic building block of our parallel coupled-line filter. The coupled line in Fig. 3(b) is the variation of Fig. 3(a). All circuit dimensions of the meandered parallel coupled line are shown in Fig. 3(b), where w is the linewidth, s is the line spacing, l is the coupled-Schiffman section length, d is the interconnecting coupled-line length, which is also called the meandered distance, and b is the tail coupled-line length. The meandered parallel coupled-line section, shown in Fig. 3(b), has the advantage of reducing the circuit size and equalizing the modal transmission phases. The effects of equalizing the modal transmission phases are originated from the coupled-Schiffman section. As discussed previously, the coupled-Schiffman section speeds up the even-mode phase velocity. In addition, because the odd-mode current distribution cannot be approximated to that of the Schiffman section, the odd-mode phase velocity is not obviously increased as the even mode. By electromagnetic (EM) simulation, the odd-mode phase velocity is found to increase very slightly.

In an attempt to easily explain, here we neglect the tiny variation of the odd-mode transmission phase caused by meandering. The main mechanism of the proposed structure is to speed up the even-mode phase velocity and to achieve the target of $\theta_e = \theta_o = 180°$ at $2f_o$. Since odd-mode transmission phase θ_o is not affected by meandering, the total length of the proposed meandered parallel coupled line is equal to that of the conventional coupled line and the total length L is chosen to be $\theta_o = 180°$ at $2f_o$. θ_e and θ_o of a conventional coupled line are shown as the hollow-triangle dashed line and the hollow-square line in Fig. 4, respectively. θ_o is smaller than θ_e, and their difference is increased proportional to frequency. Now, if the coupled-line corners and interconnecting and tail coupled line are omitted, the even-mode phase velocity of a coupled-Schiffman section with length $L/2$ is decelerated at $2f_o$ as the hollow-circle curve shown in Fig. 4. This is because the phase velocity accelerating region of a Schiffman section should be located in the region of $\theta_e < 180°$ and the most effective accelerating region is θ_e close to 90°. Therefore, in order to make the desired $2f_o$ be located in the accelerating region, the length of the coupled-Schiffman section must be shorter than $L/2$. The even-mode phase velocity accelerating effect at $2f_o$ of a shortened coupled-Schiffman section is shown as the solid-circle line in Fig. 4. The target of $\theta_e = \theta_o = 180°$ at $2f_o$ can be achieved after adding a interconnecting coupled line, three coupled-line corners, and a tail coupled line.

With the same w and s, there are multiple solutions of coupled-Schiffman section length l, interconnecting coupled-line length d, and tail coupled-line length b for $\theta_e = \theta_o = 180°$ at $2f_o$. The hollow-circle and solid-circle curves in Fig. 5 are the even-mode transmission phases of two different meandered parallel coupled lines where $\theta_e = \theta_o = 180°$ at $2f_o$ is achieved. The reason can be briefly explained that, as b is shortened, the coupled Shiffman section length l increases and the accelerating magnitude at $2f_o$ decreases. Therefore, the meandered distance d must be shortened to compensate the reduction of accelerating magnitude. Since b and d are tunable, the layout of a proposed meandered parallel coupled-line filter can be flexibly changed to obtain a desired filter's width-to-length ratio.

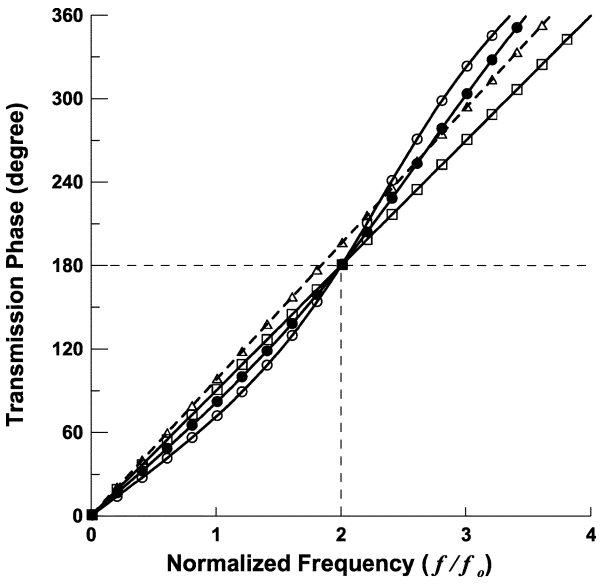

Fig. 5. Even-mode and odd-mode transmission phases of a conventional parallel coupled line, and two different solutions and of meandered parallel coupled lines with equal modal transmission phases at $2f_o$.

III. Filter Design

Design procedures of the proposed filter will now be discussed. Here, as an example, take the filter's passband frequency to be 1 GHz. Therefore, spurious passband at 2 GHz needs to be suppressed. The substrate is chosen with $\epsilon_r = 10.2$ and thickness $h = 50$ mil (1.27 mm). The main reason for choosing this relative high ϵ_r is to challenge the relatively large deviation between V_p^e and V_p^o. This will increase the difficulties in suppression of the spurious passband at $2f_o$.

As shown in Fig. 3(b), the proposed meandered parallel coupled line comprises an interconnecting coupled line, a tail coupled line, a coupled-Schiffman section, and three coupled-line corners. A circuit simulator such as Agilent ADS or AWR Microwave Office can be used to analyze the behaviors of the meandered parallel coupled line. The models used in the circuit simulation are described as following. The interconnecting and tail coupled lines use the standard microstrip coupled-line model in the circuit simulator. The coupled-line corners and coupled-Schiffman section are modeled in most of circuit simulators based on a lookup table of EM results. Using a circuit simulator can quickly get desired design parameters. Shown in Fig. 6 are the design plots of the meandered parallel coupled line obtained by the above-described circuit models. As discussed in Section II, the tail coupled line length b can be changed. Therefore, by properly choosing b, one can obtain a good length-to-width ratio of the filter. For a certain b value, two design plots such as those of Fig. 6(a) and (b) is needed to design the proposed filter. Since the dimensional and electrical variables of a meandered parallel coupled line are too many, a set of two plots to express them is required. The physical dimensions have some constrains to meet $\theta_e = \theta_o = 180°$ at $2f_o$ (this means that the physical dimensions cannot be freely chosen). To generate the design plots shown Fig. 6(a), tail coupled-line length b can be chosen first. As long as b is fixed, the meander

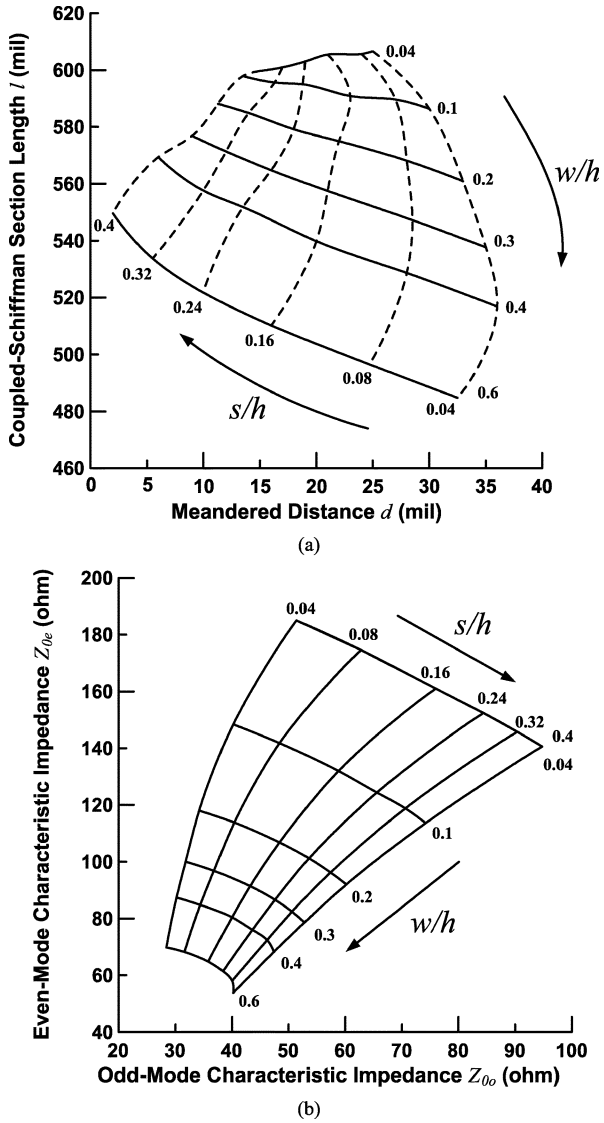

Fig. 6. Design plots of the meandered parallel coupled line with $b = 60$ mil. (a) The corresponding meandered distance d and coupled-Schiffman section length l. (b) The even- and odd-mode characteristic impedances versus w/h and s/h of a meandered parallel coupled line.

distance d and coupled-Schiffman section length l can be obtained corresponding to various w and s where the condition of $\theta_e = \theta_o = 180°$ at $2f_o$ is matched. Now all of the physical dimensions in Fig. 3(b) are fixed. We should know that, for w and s, even- and odd-mode characteristic impedances of the meandered parallel coupled line are different from that of the conventional coupled line. Fig. 6(b) shows Z_{0e} and Z_{0o} versus w and s of a meandered parallel coupled line. The particular design curves in Fig. 6 are based on b equal to a 1/80 wavelength [$\lambda/80$, i.e., approximately 60 mil (1.524 mm)]. It should be pointed out that because the accelerating magnitude around f_o is larger than $2f_o$, as shown in Fig. 5, the frequency spacing between $\theta = 90°$ and $\theta = 180°$ is smaller than one f_o. It implies that if the filter's passband frequency is at f_o, the frequency for $\theta = 180°$ at which the spurious passband located will be a little bit lower than $2f_o$.

After completing the design plots for a chosen b, we can use the design plots to design the proposed filter. First, for a given

TABLE I
FILTER DESIGN PARAMETERS

Filter	Order (n)	FBW	*b* (mil)	*w, s, d, l* of ith meandered parallel-coupled section (mil)												Overall circuit size (mil x mil)
				i=1, n+1				i=2, n				i=3, n-1				
				w	*s*	*d*	*l*	*w*	*s*	*d*	*l*	*w*	*s*	*d*	*l*	
A	3	50%	60	10	2	37	571	11	3	35	567					585 x 618
B	3	30%	60	7	5	27	600	7	8	22	605					523 x 649
C	5	50%	60	6.5	3	32	584	7	5	32	584	15	3	34	554	853 x 636

filter's passband parameters, sets of even- and odd-mode characteristic impedances of each coupled-line section are obtained based on a TEM assumption. Using Fig. 6(b), with Z_{0e} and Z_{0o} obtained in step 1, we then have the corresponding w and s. Finally, as long as w and s are known, the corresponding d and l can be obtained in Fig. 6(a). By cascading each meandered parallel coupled-line section, a proposed filter is finished. According to the previous discussion, the filter is designed with passband at f_o and is free of spurious passband at $2f_o$. The above-described design procedures based on a circuit simulator such as Agilent ADS or AWR Microwave Office can rapidly get the physical layout of the proposed filter. Final fine-tuning based on an EM simulator such as Sonnet is required to precisely eliminate the first spurious passband and to maintain the main passband performance. These design procedures can largely save the designing time compared to the method of purely using the EM simulator.

IV. SIMULATION AND MEASURED RESPONSES

Three bandpass filters with a Chebyshev response of 0.1-dB passband ripple are fabricated to demonstrate the proposed first spurious passband-free performance. The designed center frequency is 1 GHz. The circuits are fabricated on a Rogers RT/6010 substrate. The substrate has a relative dielectric constant of 10.2, a thickness of 50 mil, and a copper cladding of 0.5 oz.

Although the design procedures have been described in Section III, we still need to provide the following further explanation. Since the fractional bandwidth (FBW) of the filters is too large, design equations in [1] are not adequate. More accurate design procedures based on an ideal TEM coupled line can be used [2]. Following these design steps, a series of Z_{0e} and Z_{0o} are obtained. We can then determine if b has a preferable filter's width-to-length ratio. After b is chosen, we can draw the design plots of Fig. 6(a) and (b). Using the obtained Z_{0e} and Z_{0o} values, the corresponding w and s can then be obtained in Fig. 6(b). By using the known w and s with the design plot [see Fig. 6(a)], the corresponding d and l is, therefore, determined. The dimensions of each meandered parallel coupled-line section can be obtained separately by the above-described procedures . We can then have the circuit simulator do the initial verification for the obtained dimensions of the proposed filter. Finally, we use a EM simulator such as Sonnet to finalize the design.

Here, it must be remembered that when a circuit simulator is used, it is assumed that each meandered coupled-line section is independent of each other. The practical interaction, however, indeed exists. Since the equality of θ_e and θ_o is very sensitive to external interference, slightly tuning of d and l to compensate for interaction effects is needed in the EM simulation. Empirically, a 10% increase in d and a 5% increase in l are needed. Since the even- and odd-mode characteristic impedances are insensitive to the external interference, the w and s value can be maintained.

The parameters including the specifications and detailed dimensions of each meander parallel coupled-line section of

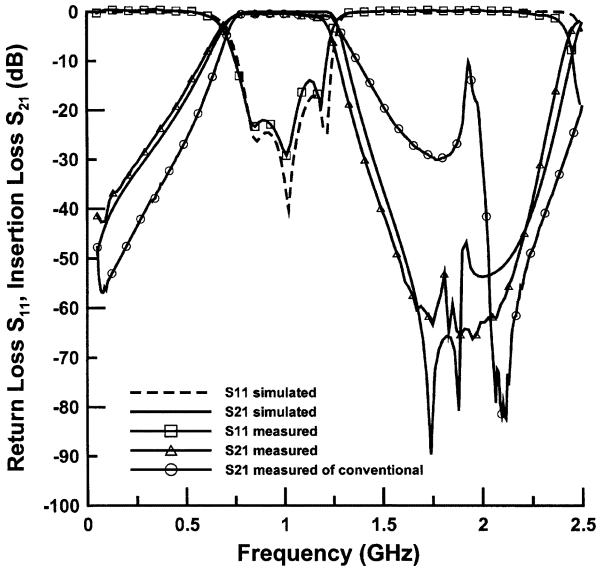

Fig. 7. Simulated and measured responses of filter A and the measured insertion loss of a conventional filter with the same specification is compared.

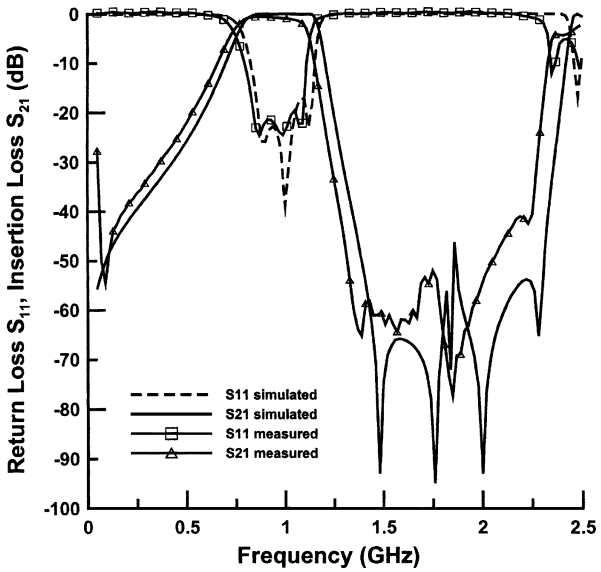

Fig. 8. Simulated and measured responses of filter B.

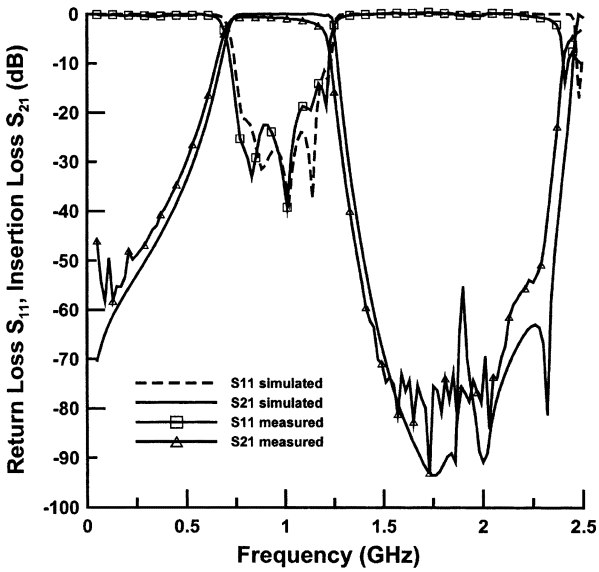

Fig. 9. Simulated and measured responses of filter C.

the filters are listed in Table I. The simulated and measured responses are depicted in Figs. 7–9, and their b are all 60 mil. Two filters with order 3 and one filter with order 5 are designed. The FBW of filter A and C (orders 3 and 5, respectively) is 50%, and that of B (order 3) is 30%. Since the lower edge of the first spurious passband is closer to the upper edge of the main passband as the filter's FBW becomes wider, the performance of the upper stopband may degrade seriously to worse than -30 dB. Therefore, a wide bandwidth filter is chosen to show the impressive improvement of the upper stopband performance. Fig. 7 shows the simulated and measured results of filter A. A conventional filter with the same specifications is also shown in Fig. 7 to compare the improvement of the upper stopband performance. In Fig. 7, the upper stopband rejection is improved from -30 dB to below -50 dB and the spurious passband suppression at 2 GHz is improved form -10 dB to below -60 dB. Comparing the proposed filter to the conventional one, an excellent improvement is achieved. In Fig. 8, filter B's upper stopband is improved to -50 dB and the spurious passband can be suppressed to approximately -55 dB. In Fig. 9, filter C's upper stopband is improved to approximately -70 dB and the spurious passband can be suppressed to approximately -70 dB. The layout of filter A is shown in Fig. 10. Fig. 11 depicts the circuit size comparison between filter A and a conventional filter with same filter parameters. It is obvious that the circuit size is drastically reduced.

V. Discussion

If we look at the simulated insertion loss of all three filters in Figs. 7–9, some transmission zeros appear in the upper stopband. These transmission zeros are possibly due to the parasitic magnetic cross-coupling between nonadjacent resonators. The parasitic magnetic coupling is because at the bottom of the filter every meandered coupled-line section has the strongest RF current, and the strongest current-carrying line segments are very close to the next meandered coupled-line sections. In the mean

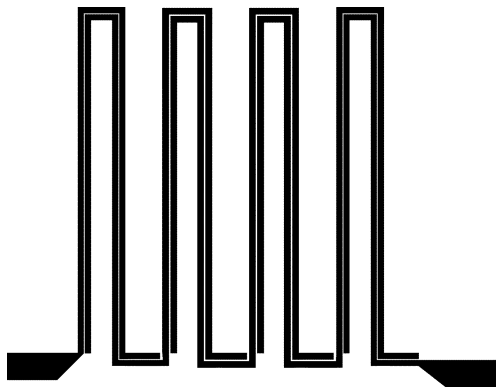

Fig. 10. Layout of filter A.

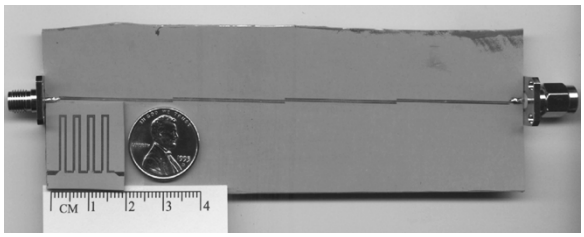

Fig. 11. Circuit size comparison between filter A and conventional filter.

time, magnetic coupling cannot be blocked by other lines. These upper stopband transmission zeros cause the filters to display a steeper upper stopband skirt than that of a lower stopband. In addition, we can observe the insertion loss at the upper end of the passband is a little bit larger than that of the lower end. The reason is because the resonator's quality factor is finite in practical fabrication and the transmissions zeros in the upper stopband cause sharp rolloff at the high side skirt. The transmission zeros are not apparent in the measured curves due to their finite resonator Q value and sensitivity of the measurement equipment (the sensitivity of our equipment is approximately -70 dB).

All the measured results have a good agreement with the simulated results in both the passband and stopband. Summarizing the above three examples, we may conservatively conclude that the proposed meandered parallel coupled filter improves the upper stopband rejection and the spurious passband at $2f_o$ by at least 20 and 40 dB, respectively.

VI. Conclusion

The proposed novel meandered parallel coupled-line structure has successfully suppressed the spurious passband at $2f_o$ and reduced the circuit size of the filter. No additional materials, components, or fabricated process are required. The idea for spurious passband suppression is based on the fact that even-mode phase velocity can be speeded up by a coupled-Schiffman section. By proper adjustment of the physical dimensions of the meandered parallel coupled-line section, an equal even- and odd-mode transmission phase at $2f_o$ can be achieved. For a desired length-to-width ratio of the filter, a proper tail coupled-line length b value can be chosen first. Furthermore, the structure can be analyzed quickly with good accuracy by a commercial circuit simulator. The design plots corresponding to a chosen b value can be easily obtained. The filter design procedures based

on this proposed structure have been described in detail. Good agreement of simulated and measured results has been achieved. Finally, the proposed filters have shown over 50-dB spurious passband suppression at $2f_o$ and a deeper upper stopband rejection than those of the conventional one.

REFERENCES

[1] S. B. Cohn, "Parallel-coupled transmission-line-resonator filters," *IRE Trans. Microw. Theory Tech.*, vol. MTT-6, no. 4, pp. 223–231, Apr. 1958.

[2] G. L. Matthaei, "Design of wide-band (and narrow-band) bandpass microwave filters on the insertion loss basis," *IRE Trans. Microw. Theory Tech.*, vol. MTT-8, no. 11, pp. 580–593, Nov. 1960.

[3] C.-Y. Chang and T. Itoh, "A modified parallel-coupled filter structure that improves the upper stopband rejection and response symmetry," *IEEE Trans. Microw. Theory Tech.*, vol. 39, no. 2, pp. 310–314, Feb. 1991.

[4] A. Riddle, "High performance parallel coupled microstrip filters," in *IEEE MTT-S Int. Microwave Symp. Dig.*, 1988, pp. 427–430.

[5] D. M. Pozar, *Microwave Engineering*, 2nd ed. New York: Wiley, 1998, pp. 474–485.

[6] J.-T. Kuo, S.-P. Chen, and M. Jiang, "Parallel-coupled microstrip filters with over-coupled end stages for suppression of spurious responses," *IEEE Microw. Wireless Compon. Lett.*, vol. 13, no. 10, pp. 440–442, Oct. 2003.

[7] B. Easter and K. A. Merza, "Parallel-coupled-line filters of invented-microstrip and suspended-substrate MIC's," in *11th Eur. Microwave Conf. Dig.*, 1981, pp. 164–167.

[8] S. L. March, "Phase velocity compensation in parallel-coupled microstrip," in *IEEE MTT-S Int. Microwave Symp. Dig.*, 1982, pp. 410–412.

[9] I. J. Bahl, "Capacitively compensated high performance parallel coupled microstrip filters," in *IEEE MTT-S Int. Microwave Symp. Dig.*, 1989, pp. 679–682.

[10] J.-T. Kuo, M. Jiang, and H.-J. Chang, "Design of parallel-coupled microstrip filters with suppression of spurious resonances using substrate suspension," *IEEE Trans. Microw. Theory Tech.*, vol. 52, no. 1, pp. 83–89, Jan. 2004.

[11] T. Lopetegi, M. A. G. Laso, J. Hernandez, M. Bacaicoa, D. Benito, M. J. Garde, M. Sorolla, and M. Guglielmi, "New microstrip 'wiggly-line' filters with spurious passband suppression," *IEEE Trans. Microw. Theory Tech.*, vol. 49, no. 9, pp. 1593–1598, Sep. 2001.

[12] C. Quendo, J. Coupez, C. Person, E. Rius, M. Roy, and S. Toutain, "Bandpass filters with self-filtering resonators: A solution to control spurious resonances," in *IEEE MTT-S Int. Microwave Symp. Dig.*, 1999, pp. 1135–1138.

[13] M. Makimoto and S. Yamashita, "Bandpass filters using parallel coupled stripline stepped impedance resonators," *IEEE Trans. Microw. Theory Tech.*, vol. MTT-28, no. 12, pp. 1413–1417, Dec. 1980.

[14] C. Wang and K. Chang, "Microstrip multiplexer with four channels for broadband system applications," *Int. J. RF Microwave Computer-Aided Eng.*, pp. 48–54, Nov. 2001.

[15] S.-M. Wang, C.-H. Chen, and C.-Y. Chang, "A study of meandered microstrip coupler with high directivity," in *IEEE MTT-S Int. Microwave Symp. Dig.*, 2003, pp. 63–66.

[16] B. M. Schiffman, "A new class of broadband microwave 90° phase shifter," *IRE Trans. Microw. Theory Tech.*, vol. MTT-6, no. 4, pp. 232–237, Apr. 1958.

Shih-Ming Wang was born in Tainan, Taiwan, R.O.C., on February 15, 1978. He received the B.S. and M.S. degrees in electrical engineering from the National Sun Yat-Sen University, Kaohsiung, Taiwan, R.O.C., in 1999 and 2001, respectively, and is currently working toward the Ph.D. degree in communication engineering at the National Chiao-Tung University.

His research interests include the analysis and design of microwave and millimeter-wave circuits.

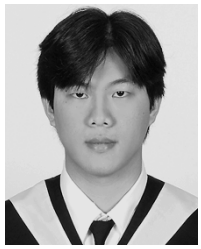

Chun-Hsiang Chi received the B.S. degree in electronic engineering from the National Sun Yet-Sen University, Kaohsiung, Taiwan, R.O.C., in 2002, and is currently working toward the M.S. degree in communication engineering at the National Chiao-Tung University.

His research interests including low-temperature co-fired ceramic (LTCC) RF passive components and LTCC modules design for wireless local area network (LAN) applications.

Ming-Yu Hsieh was born in Taiwan, R.O.C., on July 2, 1978. He received the B.S. and M.S. degrees in communication engineering from the National Chiao Tung University, Hsinchu, Taiwan, R.O.C., in 2001 and 2003, respectively.

In 2003, he joined the Chung-Shan Institute of Science and Technology (CSIST), Lung-Tang, Taiwan, R.O.C., as an RF Engineer. His research interests include microwave broad-band filter design and oscillator design.

Chi-Yang Chang (S'88–M'95) was born in Taipei, Taiwan, R.O.C., on December 20, 1954. He received the B.S. degree in physics and M.S. degree in electrical engineering from the National Taiwan University, Taiwan, R.O.C., in 1977 and 1982, respectively, and the Ph.D. degree in electrical engineering from The University of Texas at Austin, in 1990.

From 1979 to 1980, he was a Teaching Assistant with the Department of Physics, National Taiwan University. From 1982 to 1988, he was an Assistant Researcher with the Chung-Shan Institute of Science and Technology (CSIST), where he was in charge of development of microwave integrated circuits (MICs), microwave subsystems, and millimeter-wave waveguide E-plane circuits.

From 1990 to 1995, he returned to CSIST as an Associate Researcher, where he was in charge of development of uniplanar circuits, ultra-broad-band circuits, and millimeter-wave planar circuits. In 1995, he jointed the faculty of the Department of Communication, National Chiao-Tung University, Hsinchu, Taiwan, R.O.C., as an Associate Professor and, in 2002, became a Professor. His research interests include microwave and millimeter-wave passive and active circuit design, planar miniaturized filter design, and monolithic-microwave integrated-circuit (MMIC) design.